Molecular Pharmacology Fast Forward. Published on May 2, 2018 as DOI: 10.1124/mol.117.111153
This article has not been copyedited and formatted. The final version may differ from this version.

Molecular Mechanisms for Species Differences in Organic Anion Transporter 1, OAT1: Implications for Renal Drug Toxicity

Ling Zou, Adrian Stecula, Anshul Gupta, Bhagwat Prasad, Huan-Chieh Chien, Sook Wah Yee, Li Wang, Jashvant D. Unadkat, Simone H. Stahl, Katherine S. Fenner, Kathleen M. Giacomini

Department of Bioengineering and Therapeutic Sciences, University of California, San Francisco, California, 94143, United States (L.Z., A.S., H.C.C., S.W.Y., K.M.G.)

Pharmacokinetics and Drug Metabolism, Amgen Inc., Cambridge, Massachusetts, United States (A.G.)

Department of Pharmaceutics, School of Pharmacy, University of Washington, Seattle, Washington, 98195, United States (B.P., L.W., J.D.U.)

ADME Transporters, Safety and ADME Translational Sciences, Drug Safety and Metabolism IMED, AstraZeneca, Cambridge, United Kingdom (S.H.S., K.S.F.)

Molecular Pharmacology Fast Forward. Published on May 2, 2018 as DOI: 10.1124/mol.117.111153
This article has not been copyedited and formatted. The final version may differ from this version.

MOL #111153

Running title: OAT1 in antiviral drug-induced renal toxicity

Corresponding author:

Kathleen M. Giacomini, Ph.D.

Department of Bioengineering & Therapeutic Sciences

Schools of Pharmacy and Medicine

University of California San Francisco

1550 4th Street

Mission Bay, RH 584, MB2911

San Francisco, CA 94158

Email: kathy.giacomini@ucsf.edu

Tel: (415) 476-1936

Fax: (415) 514-4361

Number of text pages: 16

Number of tables: 6

Number of figures: 5

Number of references: 61

Number of words in the Abstract: 223

Number of words in the Introduction: 595

Number of words in the Discussion: 1315

Abbreviations: Organic anion transporter 1, OAT1; Acyclic nucleoside phosphonates, ANPs; 6-carboxyfluorescein, 6CF; HEK293, human embryonic kidney 293; human organic anion transporter 1, hOAT1; cynomolgus monkey organic anion transporter 1, cyOAT1; rat organic anion transporter 1, rOAT1; mouse organic anion transporter 1, mOAT1; dog organic anion transporter 1, dOAT1; SUA, serum uric acid

Molecular Pharmacology Fast Forward. Published on May 2, 2018 as DOI: 10.1124/mol.117.111153
This article has not been copyedited and formatted. The final version may differ from this version.

Abstract

Species differences in renal drug transporters continue to plague drug development with animal models failing to adequately predict renal drug toxicity. For example, adefovir, a renally excreted antiviral drug, failed clinical studies for HIV due to pronounced nephrontoxicity in humans. In this study, we demonstrated that there are large species differences in the kinetics of interactions of a key class of antiviral drugs, acyclic nucleoside phosphonates (ANPs), with OAT1 (SLC22A6) and identified a key amino acid residue responsible for these differences. In OAT1 stably transfected HEK293 cells, the K_m of tenofovir for human OAT1 was significantly lower than for OAT1 orthologs from common preclinical animals, including cynomolgus monkey, mouse, rat and dog. Chimeric and site-directed mutagenesis studies along with comparative structure modeling identified serine at position 203 (S203) in hOAT1 as a determinant of its lower K_m value. Further, S203 is conserved in apes and in contrast, alanine at the equivalent position is conserved in preclinical animals and Old World monkeys, the most related primates to apes. Intriguingly, transport efficiencies are significantly higher for OAT1 orthologs from apes with high serum uric acid levels than the orthologs from species with low serum uric acid levels. In conclusion, our data provide a molecular mechanism underlying species differences in renal accumulation of nephrotoxic ANPs and a novel insight into OAT1 transport function in primate evolution.

Molecular Pharmacology Fast Forward. Published on May 2, 2018 as DOI: 10.1124/mol.117.111153
This article has not been copyedited and formatted. The final version may differ from this version.

Introduction

Acyclic nucleoside phosphonates (including adefovir, cidofovir and tenofovir) have become a key class of antiviral drugs due to many unique features such as their prolonged action and low resistance profile(De Clercq and Holy 2005). However, nephrotoxicity remains a concern for the ANPs. For example, adefovir was not approved by FDA for the treatment of HIV infection because of pronounced nephrotoxicity at dosages of 60 mg to 120 mg per day(Mellors 1999). Subsequently, the drug was approved at 10 mg per day for the treatment of Hepatitis B infections (HBV). However, even at low doses, the drug still has the potential to cause nephrotoxicity after chronic administration particularly in patients with pre-existing kidney disease. Further, the product label for cidofovir, used in the treatment of cytomegalovirus, includes a recommendation that probenecid be co-administered with the drug. Finally, though rare, tenofovir has been associated nephrotoxicity including Fanconi Bickel Syndrome(Dahlin et al. 2015).

The mechanism for nephrotoxicity of ANPs is related to accumulation of the drugs in renal proximal tubules(De Clercq and Holy 2005). Studies suggest that cytotoxicity of these antiviral agents is increased 100-fold in cells expressing the OAT1(Ho et al. 2000). In fact, OAT1, which is highly expressed on the basolateral membrane of renal tubule epithelial cells, plays an important role in the uptake of ANPs into proximal tubular cells(De Clercq and Holy 2005, Uwai et al. 2007). OAT1-mediated accumulation of adefovir and cidofovir is associated with increased cellular toxicity in *in vitro* assays (Ho et al. 2000) and as noted, probenecid, a potent inhibitor of OAT1, reduces the nephrotoxic effects of cidofovir in both cynomolgus monkeys and humans(Lacy et al. 1998).

Thus, the question of whether preclinical animal species orthologs of OAT1 exhibit transport kinetics similar to the human orthologue becomes important for predicting nephrotoxicity in

Molecular Pharmacology Fast Forward. Published on May 2, 2018 as DOI: 10.1124/mol.117.111153
This article has not been copyedited and formatted. The final version may differ from this version.

humans. Currently, our knowledge of differences in antiviral drug transport kinetics of OAT1 among human and preclinical animal species orthologs is limited. For example, the K_m of hOAT1 for cidofovir and adefovir was found to be five-to-nine-fold lower compared with rat OAT1(Cihlar et al. 1999). On the other hand, there were minimal species differences between hOAT1 and the orthologue from cynomolgus monkey in terms of localization in the kidney, as well as its K_m and transport efficiency (V_{max}/K_m) for 11 substrates, including two antiviral drugs, acyclovir and zidovudine(Tahara et al. 2005).

Here we hypothesized that there are large species differences in the kinetics of ANP uptake into cells via OAT1, which may contribute to species differences in renal accumulation of these potentially nephrotoxic antiviral drugs. We report that hOAT1 had a significantly lower K_m value for the antiviral drug, tenofovir, in comparison to OAT1 species orthologs from four commonly used preclinical animals, including cynomolgus monkey, mouse, rat and dog. We demonstrated that S203, a residue predicted to be in the binding site of hOAT1, was essential for a lower tenofovir K_m than alanine at the equivalent position. In addition, tenofovir transport efficiency (V_{max}/K_m) was higher for hOAT1 than for orthologs from the four preclinical animal species. Finally, we explored primate evolution of the transporter, and noted that all apes consistently have S203 whereas most Old and New World monkeys have A203. One of the remarkable characteristics of apes is that they lost functional uricase during evolution(Kratzer et al. 2014) and consequently their serum uric acid levels are significantly higher than species with uricase activity. Though speculative, our data suggest that S203 in OAT1, which results in a greater efficiency of transport, evolved to aid apes in handling the higher levels of uric acid associated with the loss of uricase.

Molecular Pharmacology Fast Forward. Published on May 2, 2018 as DOI: 10.1124/mol.117.111153
This article has not been copyedited and formatted. The final version may differ from this version.

Materials and Methods

Chemicals and Reagents

Adefovir, cidofovir, 6-carboxyfluorescein and glutaric acid were purchased from Sigma-Aldrich (St. Louis, MO). Tenofovir was purchased from Carbosynth (Berkshire, United Kingdom). α-Ketoglutarate was purchased from Spectrum Chemicals & Lab Products (Gardena, CA). [^{3}H]-tenofovir and [^{14}C]-uric acid were purchased from American Radiolabeled Chemicals (St. Louis, MO). The specific activities of these compounds were 10 Ci/mmol and 50 mCi/mmol, respectively. [^{3}H]- adefovir and [^{3}H]-cidofovir were purchased from Moravek Inc. (Brea, CA). The specific activities of these compounds were 16.6 Ci/mmol and 30.5 Ci/mmol, respectively. [^{3}H]-PAH was purchased from PerkinElmer Health Sciences Inc. (Shelton, CT) with specific activity of 5 Ci/mmol. Cynomolgus monkey and dog whole kidneys were purchased from BioreclamationIVT (New York, NY). Samples of mouse and rat whole kidneys were provided by AstraZeneca (Waltham, MA).

Blast and sequence alignment. Human OAT1 amino acid sequence from 196 to 210 (GMALAGISLNCMTLN) was used to perform protein blast using the online tool BLAST(Altschul, Madden et al. 1997) (https://blast.ncbi.nlm.nih.gov/Blast.cgi?PROGRAM=blastp&PAGE_TYPE=BlastSearch&LINK_LOC=blasthome) to identify species with verified or predicted OAT1 amino acid sequences. OAT1 orthologs from proboscis monkey (*Nasalis larvatus*), hamadryas baboon (*Papio hamadryas*) *and* small-eared galago (*Otolemur garnettii*) were obtained from UCSC Genome Browser. OAT1 amino acid sequences were aligned using Clustal Omega(Goujon, McWilliam et al. 2010, Sievers, Wilm et al. 2011, McWilliam, Li et al. 2013) (http://www.ebi.ac.uk/Tools/msa/clustalo/).

Molecular Pharmacology Fast Forward. Published on May 2, 2018 as DOI: 10.1124/mol.117.111153
This article has not been copyedited and formatted. The final version may differ from this version.

Cloning and establishment of expression vectors of human, cynomolgus monkey, mouse, rat, dog, chimpanzee, gorilla, gibbon, orangutan and galago OAT1 orthologs. PCR primers (Supplemental Table 1) based on the coding regions of OAT1 of human (NM_153276.2) was designed to amplify full-length fragments from our previous work(Fujita, Brown et al. 2005). PCR primers (Supplemental Table 1) based on the coding regions of cynomolgus monkey (NM_001287697.1), rat (NM_017224.2), and dog (XM_533258.5) were designed to amplify full-length fragments from kidney cDNAs (Zyagen, San Diego, CA) from corresponding species. The coding regions of mouse Oat1 (BC021647.1) were amplified from cDNA clones purchased from OriGene (Rockville, MD). The coding sequences of OAT1 from chimpanzee (XM_001160252.4), western lowland gorilla (XM_019037481.1) and northern white-cheeked gibbon (XM_003274115.1) were generated from human OAT1 using Q5® Site-Directed Mutagenesis Kit (New England Biolabs, Ipswich, MA). Sumatran orangutan OAT1 (XM_002821628.1) and small-eared galago (XM_003798698.1) were synthesized by GenScript USA Inc. (Piscataway, NJ). OAT1 coding sequences were inserted in the pcDNA5/FRT plasmid to generate expression constructs.

Construction of chimeric transporters. Amino acid sequences of hOAT1 and cyOAT1 were aligned and 17 different amino acids were identified between the two species. Chimeric proteins were constructed using NEBuilder® HiFi DNA Assembly Cloning Kit (New England Biolabs, Ipswich, MA). Three chimeric transporters (human 1-136 + cynomolgus monkey 137-550; human 1-300 + cynomolgus monkey 301-550; cynomolgus monkey 1-400 + human 401-550) were constructed. The sequence of each chimera was confirmed by DNA sequencing (Mc Lab, South San Francisco, CA).

Cloning of human and cynomolgus monkey OAT1 mutants. Human OAT1 S203A, S203T and cynomolgus monkey OAT1 S198A, A203S, I254V and V256A were generated using Q5®

Molecular Pharmacology Fast Forward. Published on May 2, 2018 as DOI: 10.1124/mol.117.111153
This article has not been copyedited and formatted. The final version may differ from this version.

Site-Directed Mutagenesis Kit according to the manufacturer's protocol. Sequences were confirmed by DNA sequencing.

Transfection and establishment of stable cell lines. Genes encoding OAT1 orthologs and mutants were transfected in HEK293-Flp-In cells (ThermoFisher Scientific, Waltham, MA) using Lipofectamine LTX (Life Technologies, Carlsbad, CA) according to the manufacturer's protocol. HEK293-Flp-In cells stably transfected with the empty vector or the vector containing the genes of interest were grown in DMEM supplemented with 10% fetal bovine serum, penicillin (100 U/ml), streptomycin (100 µg/ml), sodium pyruvate (110 µg/ml) and hygromycin B (100 µg/ml) at 37°C in a humidified incubator with 5% CO_2.

Inhibition of human OAT1-mediated 6CF uptake by adefovir, cidofovir and tenofovir. The method is as described(Liang, Chien et al. 2015) with minor modifications. Cells were seeded in black wall poly-D-lysine-coated 96 well plates for 24 h to reach 95% confluence. Before the uptake experiment, cell culture medium was removed and the cells were washed with Hank's balanced salt solution (HBSS). The inhibition of the uptake of 1 µM 6CF by OAT1 was performed at 37°C in the presence of antiviral drugs adefovir, cidofovir and tenofovir at desired concentrations. The uptake was terminated at 1 minute. Cells were washed twice with ice-cold HBSS buffer. The IC_{50} values were calculated by GraphPad Prism software.

Transporter uptake studies. The uptake was initiated by incubating transiently or stably over-expressing cell lines with HBSS containing desired concentrations of a substrate. Cells were seeded in black wall poly-D-lysine-coated 96 well plates for 24 h to reach 95% confluence. Before the uptake experiment, cell culture medium was removed and the cells were washed with Hank's balanced salt solution (HBSS). The details for drug concentrations and uptake time are described in Results and figure legends. For the uric acid uptake assay, unlabeled uric acid

Molecular Pharmacology Fast Forward. Published on May 2, 2018 as DOI: 10.1124/mol.117.111153
This article has not been copyedited and formatted. The final version may differ from this version.

was dissolved in 0.1N NaOH and added to obtain designed concentrations in HBSS buffer plus 10 mM HEPES to maintain pH 7.4. The uptake was performed at 37 °C, and then the cells were washed three times with ice-cold HBSS. After that, the cells were lysed with lysis buffer containing 0.1 N NaOH and 0.1% SDS, and the radioactivity in the lysate was determined by liquid scintillation counting. For the transporter study, the K_m and V_{max} were calculated by fitting the data to a Michaelis–Menten equation using GraphPad Prism 7 (La Jolla, CA).

OAT1 comparative structure modeling and docking. Human OAT1 was modeled using the 2.9 Å crystal structure of a high-affinity phosphate transporter (PiPT) from *Piriformospora indica*, in an inward-facing occluded state, with bound phosphate(Pedersen, Kumar et al. 2013). The final sequence alignment was obtained by manual refinement of gaps in the output from PROMALS3D(Pei, Tang et al. 2008) and MUSCLE(Edgar 2004) web servers. One hundred models were generated using the 'automodel' class of MODELLER 9.16(Sali and Blundell 1993) and evaluated using the normalized discrete optimized protein energy (zDOPE) potential(Shen and Sali 2006). The top-scoring model was then used for the prediction of a putative binding site near the location of the crystallographic phosphate with the FTMap web server(Kozakov, Grove et al. 2015). Tenofovir was docked against the binding site with UCSF DOCK 3.6(Coleman, Carchia et al. 2013).

Membrane protein extraction and quantification. The total membrane proteins were extracted using ProteoExtract Kit (EMD Millipore, Billerica, MA). The final membrane fraction was diluted to a working concentration of 2 µg membrane protein/µl as quantified by the BCA assay. Total membrane proteins were reduced, denatured, alkylated and digested in triplicates as per our previously reported protocol(Prasad, Johnson et al. 2016). OAT1 surrogate peptide, TSLAVLGK, generated by trypsin digestion was quantified by LC-MS/MS, where the synthetic light peptide was used as the calibrator. The corresponding heavy peptide labelled at [$^{13}C_6{}^{15}N_2$]-

Molecular Pharmacology Fast Forward. Published on May 2, 2018 as DOI: 10.1124/mol.117.111153
This article has not been copyedited and formatted. The final version may differ from this version.

lysine was used as the internal standard. Peptide quantification was performed using the Waters® Xevo TQ-S tandem mass spectrometer coupled to Waters® Acquity™ UPLC system (Waters, Hertfordshire, UK). A UPLC column (Acquity UPLC® HSS T3 1.8 µm, 2.1 x 100 mm, Waters), with a Security Guard column (C18, 4 mm × 2.0 mm) from Phenomenex (Torrance, CA), was eluted (0.3 mL/min) with a gradient mobile phase consisting of water and acetonitrile (with 0.1% formic acid). The injection volume was 5 µL (~10 µg of total protein). The optimized LC-MS/MS parameters(Prasad, Johnson et al. 2016) were used in ESI positive ionization mode. The data were processed by integrating the peak areas generated from the reconstructed ion chromatograms for the analyte peptides and the respective heavy internal standards using the MassLynx software (Waters). The OAT1 protein levels in the cells expressing the OAT1 orthologs from five species were measured, however, the OAT1 protein levels from cells expressing the mutant OAT1 proteins, were not determined.

Statistical Analysis. Unless specified, data in figures and tables were expressed as mean ± standard deviation (SD). All experiments were performed at least twice with 3 to 4 replicates of each data point. Statistical analyses, as specified in the legends of the figures and tables, were performed to determine significant differences between controls and treatment groups. The data were analyzed using GraphPad Prism 7 (La Jolla, CA). A p-value <0.05 was considered statistically significant.

Molecular Pharmacology Fast Forward. Published on May 2, 2018 as DOI: 10.1124/mol.117.111153
This article has not been copyedited and formatted. The final version may differ from this version.

Results

Inhibition of OAT1-mediated 6-carboxyfluorescein (6CF) uptake by ANPs. To determine whether there are species differences in the interaction kinetics of ANPs with OAT1, we first characterized inhibition potencies of the three ANPs. Adefovir, cidofovir and tenofovir inhibited uptake of 6CF in HEK293 cells stably expressing OAT1 orthologs from five species, human (hOAT1), cynomolgus monkey (cyOAT1), rat (rOAT1), mouse (mOAT1) and dog (dOAT1) (Figure 1). Notably, the IC_{50} values of adefovir and tenofovir for hOAT1 (71 ± 15 μM and 61 ± 14 μM, respectively, Table 1) were significantly lower than the values for OAT1 orthologs from the four preclinical animal species. Importantly, the IC_{50} values of adefovir, cidofovir and tenofovir for hOAT1 was 3.1-, 2.1- and 5.6-fold, respectively, lower than the IC_{50} values for cyOAT1, which has the greatest homology to hOAT1 compared with the other species orthologs studied.

Kinetic studies of tenofovir transport by hOAT1 and four common preclinical animals. To further characterize species differences in the kinetics of the transporter for ANPs, we used [^{3}H]-tenofovir as a model substrate. We selected tenofovir for more detailed studies because of its widespread use as an antiviral agent; however, key experiments were validated with adefovir and cidofovir (Figure 3G). First, we compared the kinetics of uptake of [^{3}H]-tenofovir in the stable cell lines recombinantly expressing hOAT1 or the orthologs from the aforementioned four preclinical animals. The K_m value for hOAT1-mediated tenofovir uptake (72.6 ± 20 μM) was significantly lower than the respective K_m values for OAT1 orthologs from cynomolgus monkey, mouse, rat and dog (Table 2). Moreover, tenofovir transport efficiency (V_{max}/K_m) for hOAT1 was greater than its transport efficiency for cyOAT1 before and after normalization for total cell membrane-bound proteins (Figure 2A, Table 2). As expected, the V_{max} of tenofovir for OAT1 orthologs was significantly correlated with total cell membrane-associated quantity of OAT1 in the stable cell lines (R^2=0.89) (Figure 2B, Supplemental Table 3). It should be noted that membrane-associated protein levels of the various species orthologs of OAT1 in transfected

Molecular Pharmacology Fast Forward. Published on May 2, 2018 as DOI: 10.1124/mol.117.111153
This article has not been copyedited and formatted. The final version may differ from this version.

HEK cells may not reflect quantities of OAT1 in the kidney tissue. Thus, *in vivo* maximum transport rates and efficiencies among the OAT1 orthologs may differ from what was observed in the cell lines. In fact, we found that the total cell membrane-bound protein level for hOAT1 was the highest in transfected HEK293 cells but the lowest among all the five species in the kidney cortex (Supplemental Table 3).

Functional characterization of chimeric and mutant transporters. cyOAT1 has 96.91% amino acid identity to hOAT1 (Supplemental Table 2) and yet its K_m value for tenofovir was 3.5-fold higher than the corresponding K_m for hOAT1 (Table 2). To identify the essential domains and amino acid residues in hOAT1 responsible for the lower K_m of tenofovir, chimeric transporters between cyOAT1 and hOAT1 were created and characterized. Tenofovir uptake for chimeric transporter "hOAT1 1-300 + cyOAT1 301-550" was comparable to that for hOAT1 wildtype. In contrast, "hOAT1 1-136 + cyOAT1 137-550" and "cyOAT1 1-400 + hOAT1 401-550" were comparable to cyOAT1 wildtype (Figure 3C). These results suggested that the residues critical for the greater transport efficiency and lower K_m of tenofovir were in hOAT1 residues 136-300. Therefore, we focused on four hOAT1 residues, which differ between hOAT1 and cyOAT1 in this region, A198, S203, V254 and A256 (Figure 3A).

Expression vectors containing cyOAT1 with each of the four amino acids mutated to the corresponding amino acid in hOAT1 (S198A, A203S, I254V and V256A) were constructed and transiently over-expressed in HEK293 cells. Tenofovir uptake rate for cyOAT1 A203S was almost three times greater than that of wildtype cyOAT1 (Figure 3D), whereas no significant changes in its uptake rate were observed for the other three mutants. Next, we evaluated tenofovir transport in cells expressing the corresponding mutation in hOAT1 (S203A), which resulted in a 60% reduction in the rate of tenofovir uptake (Figure 3D). In addition, the K_m of tenofovir for hOAT1 S203A (216 ± 19 μM) was significantly higher than for hOAT1 wildtype (72

Molecular Pharmacology Fast Forward. Published on May 2, 2018 as DOI: 10.1124/mol.117.111153
This article has not been copyedited and formatted. The final version may differ from this version.

± 20 μM) whereas the K_m of tenofovir for cyOAT1 A203S (105 ± 27 μM) was significantly lower than cyOAT1 wildtype (254 ± 0.1 μM). Further, the K_m value of tenofovir for cyOAT1 A203S was not significantly different from hOAT1 wildtype (Figure 3E, Table 3). These experimental results were further supported by the docking results of tenofovir against an hOAT1 comparative structure model. The $–PO_3H_2$ moiety is shown to form a hydrogen bond with the side chain hydroxyl of S203 and Y230, thus stabilizing tenofovir within the binding site (Supplemental Figure 1) and S203A mutation eliminates this favorable interaction. These results strongly suggest that S203 in hOAT1 is important for the lower K_m of tenofovir. Notably, the uptake rates of [^{3}H]-adefovir and [^{3}H]-cidofovir for hOAT1 were significantly greater than those for cyOAT1 and hOAT1 S203A (P=0.0001). Consistently, the uptake rate of [^{3}H]-adefovir for cyOAT1 A203S was significantly higher than that for cyOAT1 (P=0.0001). In contrast, the uptake rate of [^{3}H]-cidofovir for cyOAT1 A203S was not significantly higher than that for cyOAT1 (Figure 3G). In addition, since OAT1 functions as a substrate/α-ketoglutarate exchanger (Lu, Chan et al. 1999), we measured hOAT1- and cyOAT1-mediated [^{3}H]-tenofovir uptake after pre-incubation with 5 mM α-ketoglutarate or glutaric acid for 120 min. Consistent with the previous study (Lu, Chan et al. 1999), pre-treatment with α-ketoglutarate and glutaric acid significantly increased [^{3}H]-tenofovir uptake by both hOAT1 and cyOAT1. α-Ketoglutarate pre-incubation had a greater effect on tenofovir uptake by cyOAT1 than by hOAT1 (1.45 times versus 1.95 times tenofovir uptake in the absence of α-ketoglutarate in cells expressing hOAT1 and cyOAT1, respectively). However, cyOAT1 transport activity remained significantly lower than hOAT1 transport activity after pre-incubation with α-ketoglutarate. These results suggest that α-ketoglutarate and glutaric acid stimulate the activity of OAT1 irrespective of whether an alanine or a serine is present at position 203. Additionally, an alanine at position 203 results in lower activity of OAT1 in comparison to a serine at the same position in the presence or absence of the counterion.

Molecular Pharmacology Fast Forward. Published on May 2, 2018 as DOI: 10.1124/mol.117.111153
This article has not been copyedited and formatted. The final version may differ from this version.

Comparison of K_m values of tenofovir for OAT1 orthologs with serine or alanine. Tenofovir uptake kinetics in stable cell lines recombinantly expressing OAT1 orthologs from chimpanzee, gorilla, orangutan, gibbon, squirrel monkey and galago were determined to confirm the critical role of S203 in hOAT1-mediated tenofovir uptake. The mean value of K_m (72.4 ± 20 μM) for seven OAT1 proteins with serine was significantly lower ($P<0.001$) than the respective value for six OAT1 proteins with an alanine at the equivalent position (181 ± 46 μM) (Figure 3F, Table 4).

Association of OAT1-mediated tenofovir transport efficiency (V_{max}/K_m) with serum uric acid levels. Evolutionary studies reveal that uricase was lost during primate evolution(Kratzer, Lanaspa et al. 2014) and consequently apes have significantly elevated serum uric acid levels (Table 5). We observed that the mean value of OAT1-mediated tenofovir transport efficiency (V_{max}/K_m) was significantly greater in apes (58.9 ± 8.3 μL/mg/min, N = 5) in comparison to species with much lower serum uric acid levels (16.5 ± 5.3 μL/mg/min, N = 5, $p < 0.0001$) (Figure 4A, Table 5). Intriguingly, all apes (human, chimpanzee, gorilla, orangutan, gibbon) have a S203 (Table 4). In contrast, alanine is the only amino acid at the equivalent position in twelve OAT1 orthologs from Old World monkeys, (Supplemental Table 4), which are the most closely related primates to apes. In addition, alanine is the dominant amino acid at the equivalent position in four OAT1 orthologs from New World monkeys. Importantly, *Cebus capucinus,* unlike the other three New World monkeys, maintains high serum uric acid levels similar to human and has a T203(Fanelli and Beyer 1974). [^{3}H]-Tenofovir uptake rate in transiently transfected HEK cells overexpressing hOAT1 S203T was 75% of hOAT1 wildtype and 4.2 times of cyOAT1 wildtype (Figure 4B). Further, the K_m value of uric acid for hOAT1 (571 ± 97.7 μM) was significantly lower than its K_m for cyOAT1 (1070 ± 90 μM) (Figure 5, Table 6). The differences in K_m values of ANPs between cyOAT1 and hOAT1 were much greater than the two-fold difference in K_m values for uric acid in the two species. Nevertheless, the data suggest a potentially important endogenous role of S203 in apes.

Molecular Pharmacology Fast Forward. Published on May 2, 2018 as DOI: 10.1124/mol.117.111153
This article has not been copyedited and formatted. The final version may differ from this version.

Discussion

Nephrotoxicity is a particular concern for many antiviral agents(De Clercq and Holy 2005, Izzedine et al. 2005). To ensure the safety of healthy volunteers in first-in-human clinical studies, estimation of the maximum safe starting dose is essential, and the most widely used method is based on no observable adverse effect levels in multiple preclinical animal species(Zou et al. 2012). Transporters in the solute carrier (SLC) superfamily are important determinants of tissue levels and subcellular distribution of many drugs(Leabman et al. 2003, Giacomini et al. 2010, Shima et al. 2010, Dahlin et al. 2013, Yee et al. 2013), and therefore, play a role in drug toxicities. Thus, species differences in the activity or expression of SLC transporters may lead to failure to adequately predict drug toxicities in humans. For example, differences in subcellular expression levels of the equilibrative nucleoside transporter, ENT1, between rodents and humans led to the failure to predict the mitochondrial toxicity of fialuridine in humans that resulted in several deaths and withdrawal of the drug in Phase I clinical trials(Mckenzie et al. 1995, Lee et al. 2006). In this study, we focused on OAT1 because OAT1 expression greatly enhances the cytotoxicity of ANPs(Ho et al. 2000). In addition, the apparent failure to adequately predict the pronounced nephrotoxicity of adefovir (at 120 mg) in humans from preclinical studies in animal species (Benhamou et al. 2001) motivated us further to explore species difference in OAT1.

The major finding of this study was that there are large species differences in the uptake of ANPs via OAT1 (Table1). Notably tenofovir had a significantly lower K_m for hOAT1 than for OAT1 orthologs from cynomolgus monkey, mouse, rat and dog (Table 2). Furthermore, substitution of S203 for alanine in cyOAT1 resulted in significantly greater tenofovir transport rate (Table 3). These data suggest that hOAT1 transport may mediate a greater accumulation of ANPs in human proximal tubule in comparison to OAT1 orthologs from preclinical animal species. The high correlation between V_{max} and total cell membrane-bound protein quantity

Molecular Pharmacology Fast Forward. Published on May 2, 2018 as DOI: 10.1124/mol.117.111153
This article has not been copyedited and formatted. The final version may differ from this version.

among the five species (Figure 2B, Supplemental Table 3) suggests that the turn-over rate for tenofovir by OAT1 orthologs from the five species was similar.

There have been many studies examining the molecular basis of OAT1 function, and identifying critical amino acid residues and domains of the protein responsible for substrate recognition and translocation(Tanaka et al. 2004, You 2004, Perry et al. 2006, Xu et al. 2006, Hong et al. 2007, Hong et al. 2007, Rizwan et al. 2007, Keller et al. 2011). Importantly, we report that S203 in hOAT1 is a key determinant of the lower K_m of tenofovir. Notably, compared to all the amino acid residues in hOAT1 previously reported to be involved in the transport of ANPs (R50(Bleasby et al. 2005), Y230(Perry et al. 2006), F438(Perry et al. 2006)), S203 is the only amino acid that is different between hOAT1 and the orthologs from cynomolgus monkey, mouse, rat and dog. It is worth noting that there was no significant species difference in the K_m for the canonical substrate of OAT1, PAH, between hOAT1 and cyOAT1 (Supplemental Figure 2, Supplemental Table 5), suggesting that species differences in OAT1 orthologs are substrate dependent. These results have implications for drug development as they suggest that allometric scaling may be used to predict renal accumulation of some OAT1 substrates (e.g., PAH), but not others (e.g., tenofovir).

The maximal plasma concentrations for tenofovir in both humans (range 0.72 μM to 1.0 μM, oral dose of 300 mg) and rhesus macaques (range 1.28 μM to 2.3 μM, oral dose of 30 mg) (Kearney et al. 2004, Best et al. 2015) are well below their respective Km values (Table 2) Thus, OAT1-mediated tenofovir transport into proximal tubule cells of both humans and monkeys will be inversely correlated with their respective Km values (Table 2). Though the plasma concentrations of tenofovir are somewhat lower in humans than in monkeys at therapeutic doses, a greater accumulation of tenofovir in human proximal tubule cells may be predicted based on the lower Km of tenofovir for hOAT1 (Table 2).

Molecular Pharmacology Fast Forward. Published on May 2, 2018 as DOI: 10.1124/mol.117.111153
This article has not been copyedited and formatted. The final version may differ from this version.

Though OAT1 transports tenofovir into the proximal tubule cell across the basolateral membrane, multidrug resistance protein type 4 (MRP4) transports the drug from the cell into the lumen during active tubular secretion (Ray et al. 2006). In fact, cells expressing MRP4 are 2- to 2.5-fold less susceptible to tenofovir-induced cytotoxicity. In addition, to become pharmacologically active or cytotoxic, tenofovir requires phosphorylation by intracellular nucleotide kinases (Lade et al. 2015) (Ho et al. 2000). Thus, MRP4 and nucleotide kinases, in addition to OAT1, may directly affect levels of tenofovir and other ANPs in the proximal tubule, and modulate renal toxicity.

Of particular interest is that S203 is conserved in all the apes sequenced and archived in NCBI and UCSC Genome Browser to date when this manuscript is submitted, including human, chimpanzee, pygmy chimpanzee, gorilla, orangutan and gibbon (Supplemental Table 4). In contrast, most primates and more distant species from humans have an alanine at the equivalent position. Apes lost functional uricase during evolution(Kratzer et al. 2014) and subsequently serum uric acid levels increased two to seventeen times (Table 5). Uricase is responsible for the hydrolysis of uric acid to the more water-soluble product, allantoin, in the purine degradation pathway(Motojima et al. 1988). Mammals possessing a functional uricase typically have low serum uric acid levels. 70% of daily uric acid disposal occurs via the kidneys and its excretion and reabsorption are regulated by several renal transporters(Vitart et al. 2008, So and Thorens 2010). Polymorphisms in genes encoding these transporters, such as SLC22A12, SLC2A9 and ABCG2, are associated with high serum uric acid levels and gout(Graessler et al. 2006, Vitart et al. 2008, Kolz et al. 2009, Woodward et al. 2009). It was not previously known that *SLC22A6* locus is associated with serum uric acid (SUA) levels or gout in genomewide association studies (GWAS). However, a recent GWAS in 109,029 Japanese populations (Kanai et al. 2018) showed that SNPs within *SLC22A6* locus are significantly

Molecular Pharmacology Fast Forward. Published on May 2, 2018 as DOI: 10.1124/mol.117.111153
This article has not been copyedited and formatted. The final version may differ from this version.

associated with SUA levels with the top SNP (rs148838714) at a P-value of 3.5×10^{-34} (see Supplemental Figure 4 and Supplemental Table 6). Although the function of the SNPs within this locus are not currently known, some of these SNPs within the locus are more common in Japanese populations. Future studies are needed to characterize the function of these variants and perhaps through sequencing analysis to identify causative variant that affect the SUA. Our kinetic data showing that uric acid has a lower Km for hOAT1 than for cyOAT1 (Figure 5, Table 6) show similar trends as the kinetic data for URAT1 and suggest that OAT1 with S203 potentially evolved to more efficiently transport uric acid in apes. We also note that threonine at position 203, which is present in OAT1 from C*ebus capucinus imitator, an old world monkey that* maintains high serum uric acid levels (Fanelli and Beyer 1974) results in similar transport efficiency as serine at the equivalent position (Figure 4B). Thus, either a serine or a threonine may suffice at position 203 to confer a greater OAT1 transport efficiency. The data are consistent with the evolution of alanine to serine or threonine in OAT1 to accommodate high levels of uric acid.

In conclusion, our study indicates that there are large species differences in the kinetics of interaction of OAT1 for ANPs. S203 contributes to the lower K_m of tenofovir and uric acid for hOAT1, suggesting a novel molecular mechanism underlying species difference in the kinetics of interaction of OAT1 with ANPs. Further, S203 is conserved in apes with loss of uricase and subsequent elevated serum uric acid levels, suggesting a potentially important role in uric acid excretion and in primate evolution. Finally, our results suggest that typical species used in preclinical toxicology studies may not recapitulate OAT1-mediated drug accumulation in the kidney, resulting in a poor ability to predict nephrotoxicity for drugs that are substrates of OAT1.

Molecular Pharmacology Fast Forward. Published on May 2, 2018 as DOI: 10.1124/mol.117.111153
This article has not been copyedited and formatted. The final version may differ from this version.

Authorship Contributions

Participated in research design: Giacomini, Zou, Gupta, Stecula, Stahl, Fenner

Conducted experiments: Zou, Stecula, Chien, Wang, Prasad

Contributed new reagents or analytic tools: Unadkat

Performed data analysis: Giacomini, Zou, Stecula, Gupta, Yee, Prasad

Wrote or contributed to the writing of the manuscript: Giacomini, Zou, Stecula, Gupta, Unadkat, Prasad, Stahl, Fenner

Molecular Pharmacology Fast Forward. Published on May 2, 2018 as DOI: 10.1124/mol.117.111153
This article has not been copyedited and formatted. The final version may differ from this version.

References

Altschul SF, Madden TL, Schaffer AA, Zhang J, Zhang Z, Miller W, and Lipman DJ (1997). "Gapped BLAST and PSI-BLAST: a new generation of protein database search programs." *Nucleic Acids Res* **25**(17): 3389-3402.

Benhamou Y, Bochet M, Thibault V, Calvez V, Fievet MH, Vig P, Gibbs CS, Brosgart C, Fry J, Namini H, Katlama C, and Poynard T (2001). "Safety and efficacy of adefovir dipivoxil in patients co-infected with HIV-1 and lamivudine-resistant hepatitis B virus: an open-label pilot study." *Lancet* **358**(9283): 718-723.

Best BM, Burchett S, Li H, Stek A, Hu C, Wang J, Hawkins E, Byroads M, Watts DH, Smith E, Fletcher CV, Capparelli EV, Mirochnick M; International Maternal Pediatric and Adolescent AIDS Clinical Trials (IMPAACT) P1026s Team (2015). "Pharmacokinetics of tenofovir during pregnancy and postpartum." *HIV Med* **16**(8): 502-511.

Bleasby K, Hall LA, Perry JL, Mohrenweiser HW, and Pritchard JB (2005). "Functional consequences of single nucleotide polymorphisms in the human organic anion transporter hOAT1 (SLC22A6)." *J Pharmacol Exp Ther* **314**(2): 923-931.

Cihlar T, Lin DC, Pritchard JB, Fuller MD, Mendel DB, and Sweet DH (1999). "The antiviral nucleotide analogs cidofovir and adefovir are novel substrates for human and rat renal organic anion transporter 1." *Mol Pharmacol* **56**(3): 570-580.

Coleman RG, Carchia M, Sterling T, Irwin JJ, and Shoichet BK (2013). "Ligand pose and orientational sampling in molecular docking." *PLoS One* **8**(10): e75992.

Dahlin A. Geier E, Stocker SL, Cropp CD, Grigorenko E, Bloomer M, Siegenthaler J, Xu L, Basile AS, Tang-Liu DD, and Giacomini KM (2013). "Gene expression profiling of transporters in the solute carrier and ATP-binding cassette superfamilies in human eye substructures." *Mol Pharm* **10**(2): 650-663.

Dahlin A, Wittwer M, de la Cruz M, Woo JM, Bam R, Scharen-Guivel V, Flaherty J, Ray AS, Cihlar T, Gupta SK, and Giacomini KM (2015). "A pharmacogenetic candidate gene study of tenofovir-associated Fanconi syndrome." *Pharmacogenet Genomics* **25**(2): 82-92.

De Clercq E and Holy A (2005). "Acyclic nucleoside phosphonates: a key class of antiviral drugs." *Nat Rev Drug Discov* **4**(11): 928-940.

Edgar RC (2004). "MUSCLE: multiple sequence alignment with high accuracy and high throughput." *Nucleic Acids Res* **32**(5): 1792-1797.

Fanelli GM and Beyer KH (1974). "Uric acid in nonhuman primates with special reference to its renal transport." *Annu Rev Pharmacol Toxicol* **14**: 355-364.

Fujita T, Brown C, Carlson EJ, Taylor T, de la Cruz M, Johns SJ, Stryke D, Kawamoto M, Fujita K, Castro R, Chen CW, Lin ET, Brett CM, Burchard EG, Ferrin TE, Huang CC, Leabman MK, and Giacomini KM (2005). "Functional analysis of polymorphisms in the organic anion transporter, SLC22A6 (OAT1)." *Pharmacogenet Genomics* **15**(4): 201-209.

Goujon M, McWilliam H, Li W, Valentin F, Squizzato S, Paern J and Lopez R (2010). "A new bioinformatics analysis tools framework at EMBL-EBI." *Nucleic Acids Res* **38**: W695-W699.

Graessler J, Graessler A, Unger S, Kopprasch S, Tausche AK, Kuhlisch E, and Schroeder HE (2006). "Association of the human urate transporter 1 (hURAT1) with reduced renal uric acid excretion and hyperuricemia in a German Caucasian population." *Ann Rheum Dis* **65**: 290-290.

Ho ES, Lin DC, Mendel DB, and Cihlar T (2000). "Cytotoxicity of antiviral nucleotides adefovir and cidofovir is induced by the expression of human renal organic anion transporter 1." *J Am Soc Nephrol* **11**(3): 383-393.

Hong M, Tanaka K, Pan Z, Ma J, and You G (2007). "Determination of the external loops and the cellular orientation of the N- and the C-termini of the human organic anion transporter hOAT1." *Biochem J* **401**(2): 515-520.

Hong M, Zhou F, Lee K, and You G (2007). "The putative transmembrane segment 7 of human organic anion transporter hOAT1 dictates transporter substrate binding and stability." *J Pharmacol Exp Ther* **320**(3): 1209-1215.

International Transporter Consortium, Giacomini KM, Huang SM, Tweedie DJ, Benet LZ, Brouwer KL, Chu X, Dahlin A, Evers R, Fischer V, Hillgren KM, Hoffmaster KA, Ishikawa T, Keppler D, Kim RB, Lee CA, Niemi M, Polli JW, Sugiyama Y, Swaan PW, Ware JA, Wright SH, Yee SW, Zamek-Gliszczynski MJ, and Zhang L (2010). "Membrane transporters in drug development." *Nat Rev Drug Discov* **9**(3): 215-236.

Izzedine H, Launay-Vacher V, and Deray G (2005). "Antiviral drug-induced nephrotoxicity." *Am J Kidney Dis* **45**(5): 804-817.

Kanai M, Akiyama M, Takahashi A, Matoba N, Momozawa Y, Ikeda M, Iwata N, Ikegawa S, Hirata M, Matsuda K, Kubo M, Okada Y, and Kamatani Y (2018). "Genetic analysis of quantitative traits in the Japanese population links cell types to complex human diseases." *Nat Genet* doi: 10.1038/s41588-018-0047-6.

Kearney BP, Flaherty JF, and Shah J (2004). "Tenofovir disoproxil fumarate: clinical pharmacology and pharmacokinetics." *Clin Pharmacokinet* **43**(9): 595-612.

Keller T, Egenberger B, Gorboulev V, Bernhard F, Uzelac Z, Gorbunov D, Wirth C, Koppatz S, Dotsch V, Hunte C, Sitte HH, and Koepsell H (2011). "The large extracellular loop of organic cation transporter 1 influences substrate affinity and is pivotal for oligomerization." *J Biol Chem* **286**(43): 37874-37886.

Kolz M, Johnson T, Sanna S, Teumer A, Vitart V, Perola M, Mangino M, Albrecht E, Wallace C, Farrall M, Johansson A, Nyholt DR, Aulchenko Y, Beckmann JS, Bergmann S, Bochud M, Brown M, Campbell H; EUROSPAN Consortium, Connell J, Dominiczak A, Homuth G, Lamina C, McCarthy MI; ENGAGE Consortium, Meitinger T, Mooser V, Munroe P, Nauck M, Peden J, Prokisch H, Salo P, Salomaa V, Samani NJ, Schlessinger D, Uda M, Volker U, Waeber G, Waterworth D, Wang-Sattler R, Wright AF, Adamski J, Whitfield JB, Gyllensten U, Wilson JF, Rudan I, Pramstaller P, Watkins H; PROCARDIS Consortium, Doering A, Wichmann HE; KORA Study, Spector TD, Peltonen L, Volzke H, Nagaraja R, Vollenweider P, Caulfield M; WTCCC, Illig T, Gieger C (2009). "Meta-analysis of 28,141 individuals identifies common variants within five new loci that influence uric acid concentrations." *PLoS Genet* **5**(6): e1000504.

Kozakov D, Grove LE, Hall DR, Bohnuud T, Mottarella SE, Luo L, Xia B, Beglov D, and Vajda S (2015). "The FTMap family of web servers for determining and characterizing ligand-binding hot spots of proteins." *Nat Protoc* **10**(5): 733-755.

Kratzer JT, Lanaspa MA, Murphy MN, Cicerchi C, Graves CL, Tipton PA, Ortlund EA, Johnson RJ, and Gaucher EA (2014). "Evolutionary history and metabolic insights of ancient mammalian uricases." *Proc Natl Acad Sci U S A* **111**(10): 3763-3768.

Lacy SA, Hitchcock MJ, Lee WA, Tellier P, and Cundy KC (1998). "Effect of oral probenecid coadministration on the chronic toxicity and pharmacokinetics of intravenous cidofovir in cynomolgus monkeys." *Toxicol Sci* **44**(2): 97-106.

Lade JM, To EE, Hendrix CW, and Bumpus NN (2015). "Discovery of genetic variants of the kinases that activate tenofovir in a compartment-specific manner." *EBioMedicine* **2**(9): 1145-1152.

Leabman MK, Huang CC, DeYoung J, Carlson EJ, Taylor TR, de la Cruz M, Johns SJ, Stryke D, Kawamoto M, Urban TJ, Kroetz DL, Ferrin TE, Clark AG, Risch N, Herskowitz I, Giacomini KM; Pharmacogenetics Of Membrane Transporters Investigators (2003). "Natural variation in human membrane transporter genes reveals evolutionary and functional constraints." *Proc Natl Acad Sci U S A* **100**(10): 5896-5901.

Lee EW, Lai Y, Zhang H, and Unadkat JD (2006). "Identification of the mitochondrial targeting signal of the human equilibrative nucleoside transporter 1 (hENT1): implications for interspecies differences in mitochondrial toxicity of fialuridine." *J Biol Chem* **281**(24): 16700-16706.

Liang X, Chien HC, Yee SW, Giacomini MM, Chen EC, Piao M, Hao J, Twelves J, Lepist EI, Ray AS, and Giacomini KM (2015). "Metformin is a substrate and inhibitor of the human thiamine transporter, THTR-2 (SLC19A3)." *Mol Pharm* **12**(12): 4301-4310.

Lu JJ, Jia BJ, Yang L, Zhang W, Dong X, Li P, and Chen J (2016). "Ultra-high performance liquid chromatography with ultraviolet and tandem mass spectrometry for simultaneous determination of metabolites in purine pathway of rat plasma." *J Chromatogr B Analyt Technol Biomed Life Sci* **1036-1037**: 84-92.

Lu R, Chan BS, and Schuster VL (1999). "Cloning of the human kidney PAH transporter: narrow substrate specificity and regulation by protein kinase C." *Am J Physiol* **276**(2 Pt 2): F295-303.

Mazzali M, Hughes J, Kim YG, Jefferson JA, Kang DH, Gordon KL, Lan HY, Kivlighn S, and Johnson RJ (2001). "Elevated uric acid increases blood pressure in the rat by a novel crystal-independent mechanism." *Hypertension* **38**(5): 1101-1106.

Mckenzie R, Fried MW, Sallie R, Conjeevaram H, Di Bisceglie AM, Park Y, Savarese B, Kleiner D, Tsokos M, Luciano C, Pruett T, Stotka JL, Straus SE, and Hoofnagle JH (1995). "Hepatic failure and lactic acidosis due to fialuridine (FIAU), an investigational nucleoside analog for chronic hepatitis B." *N Engl J Med* **333**(17): 1099-1105.

McWilliam H, Li W, Uludag M, Squizzato S, Park YM, Buso N, Cowley AP, and Lopez R (2013). "Analysis tool web services from the EMBL-EBI." *Nucleic Acids Res* **41**(W1): W597-W600.

Mellors JW (1999). "Adefovir for the treatment of HIV infection: if not now, when?" *JAMA* **282**(24): 2355-2356.

Miller GE, Danzig LS, and Talbott JH (1951). "Urinary excretion of uric acid in the Dalmatian and non-Dalmatian dog following administration of diodrast, sodium salicylate and a mercurial diuretic." *Am J Physiol* **164**(1): 155-158.

Motojima K, Kanaya S, and Goto S (1988). "Cloning and Sequence Analysis of cDNA for Rat Liver Uricase." *J Biol Chem* **263**(32): 16677-16681.

Pedersen BP, Kumar H, Waight AB, Risenmay AJ, Roe-Zurz Z, Chau BH, Schlessinger A, Bonomi M, Harries W, Sali A, Johri AK, and Stroud RM (2013). "Crystal structure of a eukaryotic phosphate transporter." *Nature* **496**(7446): 533-536.

Pei J, Tang M, and Grishin NV (2008). "PROMALS3D web server for accurate multiple protein sequence and structure alignments." *Nucleic Acids Res* **36**: W30-W34.

Perry JL, Dembla-Rajpal N, Hall LA, and Pritchard JB (2006). "A three-dimensional model of human organic anion transporter 1: aromatic amino acids required for substrate transport." *J Biol Chem* **281**(49): 38071-38079.

Prasad B, Johnson K, Billington S, Lee C, Chung GW, Brown CD, Kelly EJ, Himmelfarb J, and Unadkat JD (2016). "Abundance of drug transporters in the human kidney cortex as quantified by quantitative targeted proteomics." *Drug Metab Dispos* **44**(12): 1920-1924.

Ray AS, Cihlar T, Robinson KL, Tong L, Vela JE, Fuller MD, Wieman LM, Eisenberg EJ, and Rhodes GR (2006). "Mechanism of active renal tubular efflux of tenofovir." *Antimicrob Agents Chemother* **50**(10): 3297-3304.

Rizwan AN, Krick W, and Burckhardt G (2007). "The chloride dependence of the human organic anion transporter 1 (hOAT1) is blunted by mutation of a single amino acid." *J Biol Chem* **282**(18): 13402-13409.

Sali A and Blundell TL (1993). "Comparative protein modelling by satisfaction of spatial restraints." *J Mol Biol* **234**(3): 779-815.

Shen MY and Sali A (2006). "Statistical potential for assessment and prediction of protein structures." *Protein Sci* **15**(11): 2507-2524.

Shima JE, Komori T, Taylor TR, Stryke D, Kawamoto M, Johns SJ, Carlson EJ, Ferrin TE, and Giacomini KM (2010). "Genetic variants of human organic anion transporter 4 demonstrate altered transport of endogenous substrates." *Am J Physiol Renal Physiol* **299**(4): F767-775.

Sievers F, Wilm A, Dineen D, Gibson TJ, Karplus K, Li W, Lopez R, McWilliam H, Remmert M, Soding J, Thompson JD, and Higgins DG (2011). "Fast, scalable generation of high-quality protein multiple sequence alignments using Clustal Omega." *Mol Syst Biol* **7**:539.

So A and Thorens B (2010). "Uric acid transport and disease." *J Clin Invest* **120**(6): 1791-1799.

Tahara H, Shono M, Kusuhara H, Kinoshita H, Fuse E, Takadate A, Otagiri M, and Sugiyama Y (2005). "Molecular cloning and functional analyses of OAT1 and OAT3 from cynomolgus monkey kidney." *Pharm Res* **22**(4): 647-660.

Tan PK, Farrar JE, Gaucher EA, and Miner JN (2016). "Coevolution of URAT1 and uricase during primate evolution: implications for serum urate homeostasis and gout." *Mol Biol Evol* **33**(9): 2193-2200.

Tanaka K, Zhou F, Kuze K, and You G (2004). "Cysteine residues in the organic anion transporter mOAT1." *Biochem J* **380**(Pt 1): 283-287.

Uwai Y, Ida H, Tsuji Y, Katsura T, and Inui K (2007). "Renal transport of adefovir, cidofovir, and tenofovir by SLC22A family members (hOAT1, hOAT3, and hOCT2)." *Pharm Res* **24**(4): 811-815.

Vitart V, Rudan I, Hayward C, Gray NK, Floyd J, Palmer CN, Knott SA, Kolcic I, Polasek O, Graessler J, Wilson JF, Marinaki A, Riches PL, Shu X, Janicijevic B, Smolej-Narancic N, Gorgoni B, Morgan J, Campbell S, Biloglav Z, Barac-Lauc L, Pericic M, Klaric IM, Zgaga L, Skaric-Juric T, Wild SH, Richardson WA, Hohenstein P, Kimber CH, Tenesa A, Donnelly LA, Fairbanks LD, Aringer M, McKeigue PM, Ralston SH, Morris AD, Rudan P, Hastie ND, Campbell H, and Wright AF (2008). "SLC2A9 is a newly identified urate transporter influencing serum urate concentration, urate excretion and gout." *Nat Genet* **40**(4): 437-442.

Woodward OM, Kottgen A, Coresh J, Boerwinkle E, Guggino WB, and Kottgen M (2009). "Identification of a urate transporter, ABCG2, with a common functional polymorphism causing gout." *Proc Natl Acad Sci U S A* **106**(25): 10338-10342.

Wu X, Wakamiya M, Vaishnav S, Geske R, Montgomery C Jr, Jones P, Bradley A, and Caskey CT (1994). "Hyperuricemia and urate nephropathy in urate oxidase-deficient mice." *Proc Natl Acad Sci U S A* **91**(2): 742-746.

Xu W, Tanaka K, Sun AQ, and You G (2006). "Functional role of the C terminus of human organic anion transporter hOAT1." *J Biol Chem* **281**(42): 31178-31183.

Yee SW, Nguyen AN, Brown C, Savic RM, Zhang Y, Castro RA, Cropp CD, Choi JH, Singh D, Tahara H, Stocker SL, Huang Y, Brett CM, and Giacomini KM (2013). "Reduced renal clearance of cefotaxime in asians with a low-frequency polymorphism of OAT3 (SLC22A8)." *J Pharm Sci* **102**(9): 3451-3457.

You G (2004). "Towards an understanding of organic anion transporters: structure-function relationships." *Med Res Rev* **24**(6): 762-774.

Zou P, Yu Y, Zheng N, Yang Y, Paholak HJ, Yu LX, and Sun D (2012). "Applications of human pharmacokinetic prediction in first-in-human dose estimation." *AAPS J* **14**(2): 262-281.

Molecular Pharmacology Fast Forward. Published on May 2, 2018 as DOI: 10.1124/mol.117.111153
This article has not been copyedited and formatted. The final version may differ from this version.

Footnotes

Funding for this project was provided by ASTRAZENECA UK Ltd. and the National Institutes of Health Grant [R01-DK103729] (K.M.G.).

Molecular Pharmacology Fast Forward. Published on May 2, 2018 as DOI: 10.1124/mol.117.111153
This article has not been copyedited and formatted. The final version may differ from this version.

Legends for Figures

Figure 1. Species differences in the inhibition potencies of acyclic nucleoside phosphonates, adefovir, cidofovir and tenofovir, for OAT1-mediated 6CF uptake. HEK293 cells stably expressing hOAT1, cyOAT1, rOAT1, mOAT1 and dOAT1 were incubated with HBSS buffer containing 6CF (1 μM) for 1 min with or without designed concentrations of adefovir, cidofovir and tenofovir. Data points represent the mean ± SD of 6CF uptake from three replicate determinations in a single experiment. The experiments were repeated three times and similar results were obtained. Representative curves of the OAT1-mediated 6CF uptake inhibition by acyclic nucleoside phosphonates: (A) Adefovir; (B) Cidofovir; (C) Tenofovir. IC_{50} values for each of the analogs with each OAT1 orthologue are listed in Table 1.

Figure 2. Kinetics of uptake of tenofovir for species orthologs of OAT1. (A) The uptake kinetics of [^{3}H]-tenofovir in HEK293 cells expressing hOAT1, cyOAT1, rOAT1, mOAT1 and dOAT1. Uptake rate was evaluated at 3 minutes. Each point represents the mean ± SD uptake in the OAT1 transfected cells minus that in empty vector cells. (B) Correlation of V_{max} of OAT1-mediated tenofovir uptake in HEK293 cells stably expressing five OAT1 species orthologs with total cell membrane-bound OAT1 protein quantity (R^2=0.892).

Figure 3. Chimera proteins of OAT1 created to assess the critical domains and residues involved in the species differences of tenofovir kinetics in cells stably expressing hOAT1 and cyOAT1. (A) Predicted membrane-bound hOAT1 structure showing 550 amino acids. The white color indicates amino acid residues that are conserved between hOAT1 and cyOAT1. The turquoise color shows residues that vary between hOAT1 and cyOAT1 and the orange color indicates residues that were mutated and evaluated for tenofovir transport kinetics. (B) Wildtype hOAT1, cyOAT1 and chimeric proteins with different combinations of hOAT1 and cyOAT1 amino acids. (C) [^{3}H]-tenofovir uptake by OAT1 chimera proteins. Transiently transfected HEK293 cells over-expressing chimera proteins were incubated with [^{3}H]-tenofovir (50 nM) for 3

Molecular Pharmacology Fast Forward. Published on May 2, 2018 as DOI: 10.1124/mol.117.111153
This article has not been copyedited and formatted. The final version may differ from this version.

min. (D) [^{3}H]-tenofovir uptake by cyOAT1 mutants (cyOAT1 S198A, A203S, I254V, V256A) and hOAT1 mutant (hOAT1 S203A). Transiently transfected HEK293 cells over-expressing mutant proteins were incubated with [^{3}H]-tenofovir (50 nM) for 3 min. (E) Eadie-Hofstee plot for the [^{3}H]-tenofovir uptake by stable cell lines over-expressing hOAT1 and cyOAT1 and their mutants, hOAT1 S203A and cyOAT1 A203S. (F) Comparison of the averaged K_m values for OAT1 orthologs with S203 (N=7, including human, chimpanzee, gorilla, orangutan, gibbon, galago, cynomolgus monkey OAT1 A203S) with that for OAT1 orthologs with alanine at the equivalent position (N=6, including cynomolgus monkey, squirrel monkey, mouse, rat, dog, human OAT1 S203A). Student's t-test was performed to determine significant differences between the two groups. (G) The uptake rate of [^{3}H]-adefovir and [^{3}H]-cidofovir in cells over-expressing hOAT1 and cyOAT1 and the mutants, hOAT1 S203A and cyOAT1 A203S. Each column represents the mean ± SD uptake in the OAT1 transfected cells minus that in empty vector cells. Two experiments were conducted and there were four replicates for each experiment. Statistical analyses were performed by one-way ANOVA followed by Tukey's multiple comparisons test to determine significant differences between controls and treatment groups. (H) The rate of uptake of [^{3}H]-tenofovir in HEK293 cells over-expressing hOAT1 or cyOAT1 with or without 120 min pre-incubation with 5 mM α-ketoglutarate or 5 mM glutaric acid. Each bar represents uptake (mean ± SD) in the OAT1 transfected cells minus that in empty vector cells (N≥2). * p-value < 0.05. ** p-value < 0.01. *** p-value < 0.001. **** p-value = 0.0001. n.s., not significant.

Figure 4. Association of OAT1-mediated tenofovir transport efficiency (V_{max}/K_m) with serum uric acid levels and effect of amino acid substitutions in human OAT1 on tenofovir uptake rate. (A) Mean ± SD of serum uric acid levels (black bar) and OAT1-mediated tenofovir transport efficiencies (grey bar) in species with (cynomolgus monkey, squirrel monkey, mouse, rat and dog) and without (human, chimpanzee, gorilla, orangutan, gibbon) functional uricase. * represents comparison of serum uric acid levels in species with and without uricase. #

Molecular Pharmacology Fast Forward. Published on May 2, 2018 as DOI: 10.1124/mol.117.111153
This article has not been copyedited and formatted. The final version may differ from this version.

represents comparison of tenofovir transport efficiencies in species with and without uricase. ** $p < 0.01$, #### $p < 0.0001$. (B) [^{3}H]-tenofovir uptake by hOAT1, cyOAT1 and mutants (hOAT1 S203T and hOAT1 S203A). Transiently transfected HEK293 cells over-expressing wildtype or mutant proteins were incubated with [^{3}H]-tenofovir (50 nM) for 3 min. Transporter-mediated tenofovir uptake was obtained after subtracting the respective rate of uptake in empty vector cells.

Figure 5. Uric acid uptake in HEK293 cells expressing hOAT1 or cyOAT1 as a function of time and concentration. (A) Uptake of [^{14}C]-uric acid (20 μM) as a function of time in cells expressing hOAT1 and in empty vector cells. (B) Kinetics of [^{14}C]-uric acid uptake by hOAT1 and cyOAT1. HEK293 cells over-expressing hOAT1 and cyOAT1 were incubated with [^{14}C]-uric acid (20 μM) with various concentrations of unlabeled uric acid for 5 min. Stock of uric acid was dissolved in 0.1N NaOH and added to obtain designed concentrations in HBSS buffer plus 10 mM HEPES to maintain pH 7.4. Each point represents the uptake in OAT1 expressing cells minus that in empty vector cells.

Molecular Pharmacology Fast Forward. Published on May 2, 2018 as DOI: 10.1124/mol.117.111153
This article has not been copyedited and formatted. The final version may differ from this version.

Tables

Table 1. Potencies of ANPs in inhibiting 6CF uptake by OAT1 species orthologs from human, cynomolgus monkey, mouse, rat and dog.

Inhibitor	IC_{50} (μM)				
	Human	Cynomolgus Monkey	Mouse	Rat	Dog
Adefovir	71 ± 15	220 ± 67*	399 ± 147***	263 ± 66*	181 ± 4
Cidofovir	88 ± 25	181 ± 67	237 ± 69**	245 ± 19**	185 ± 27
Tenofovir	61 ± 14	343 ± 40****	165 ± 27*	153 ± 17	223 ± 64**

N≥2. Statistical analyses were performed by one-way ANOVA followed by Dunnett's multiple comparisons test. * $P < 0.05$; ** $P < 0.01$; *** $P < 0.001$; **** $P < 0.0001$

Molecular Pharmacology Fast Forward. Published on May 2, 2018 as DOI: 10.1124/mol.117.111153
This article has not been copyedited and formatted. The final version may differ from this version.

Table 2. Kinetic parameters of the tenofovir uptake by OAT1 species orthologs from human, cynomolgus monkey, mouse, rat and dog.

	Human	Cynomolgus Monkey	Mouse	Rat	Dog
K_m (μM)	72.6 ± 20	254 ± 0.1****	138 ± 18***	139 ± 7.6***	157 ± 8.8****
V_{max} (nmol/mg/min)	4.6 ± 1.4	2.5 ± 0.2	2.4 ± 0.6*	2.1 ± 0.6*	3.9 ± 0.9
V_{max}/K_m (μL/mg/min)	63	10	17	15	25
Normalized V_{max}/K_m (μL/mg/min)[&]	1.62	0.47	1.17	2.59	0.88

N≥2. Statistical analyses were performed by one-way ANOVA followed by Dunnett's multiple comparisons test. * $P < 0.05$; *** $P < 0.001$; **** $P < 0.0001$. &, tenofovir transport efficiency for OAT1 from each species was normalized to the corresponding membrane-bound OAT1 quantity (Supplemental Table 3).

Molecular Pharmacology Fast Forward. Published on May 2, 2018 as DOI: 10.1124/mol.117.111153
This article has not been copyedited and formatted. The final version may differ from this version.

Table 3. Kinetic parameters for OAT1-mediated uptake by wildtype and mutant transporters. Mutations were created by site-directed mutagenesis of both hOAT1 and cyOAT1 at position 203.

	Human	Cynomolgus Monkey	Cynomolgus monkey A203S	Human S203A
K_m (μM)	72.6 ± 20	254 ± 0.1****	105 ± 27###	216 ± 19***
V_{max} (nmol/mg/min)	4.6 ± 1.4	2.5 ± 0.2	2.8 ± 0.1	3.6 ± 0.7
V_{max}/K_m (μL/mg/min)	63	10	27	17

N≥2. Statistical analyses were performed by one-way ANOVA followed by Tukey's multiple comparisons test. * represents comparison with human. # represents comparison between cynomolgus monkey and cynomolgus monkey A203S. **** $P < 0.0001$. ### $P < 0.001$.

Molecular Pharmacology Fast Forward. Published on May 2, 2018 as DOI: 10.1124/mol.117.111153
This article has not been copyedited and formatted. The final version may differ from this version.

Table 4. Kinetic parameters of tenofovir uptake rate by OAT1 wildtype transporters, and mutants at position 203.

Species	Amino acid at position 203 or equivalent position	K_m (μM)
Human	S	72.6 ± 20
Chimpanzee	S	44.2 ± 1.5
Gorilla	S	56.0 ± 7.5
Orangutan	S	79.0 ± 16
Gibbon	S	65.0 ± 2.4
Galago	S	84.9 ± 24
Cynomolgus monkey OAT1 A203S	S	105 ± 27
Cynomolgus monkey	A	254 ± 0.1
Squirrel monkey	A	181 ± 60
Mouse	A	138 ± 18
Rat	A	139 ± 7.6
Dog	A	157 ± 8.8
Human OAT1 S203A	A	216 ± 19

Molecular Pharmacology Fast Forward. Published on May 2, 2018 as DOI: 10.1124/mol.117.111153
This article has not been copyedited and formatted. The final version may differ from this version.

Table 5. OAT1-mediated tenofovir transport efficiencies and serum uric acid levels in species with or without functional uricase.

Species	Without uricase activity		With uricase activity	
	SUA (μM)*	Tenofovir transport efficiency (μL/mg/min)	SUA (μM)*	Tenofovir transport efficiency (μL/mg/min)
Human	318 (210 - 420)(Tan, Farrar et al. 2016)	63	--	--
Chimpanzee	244 (120 - 360)(Fanelli and Beyer 1974)	61	--	--
Gorilla	146 (130 - 160)(Fanelli and Beyer 1974)	49	--	--
Orangutan	140 (110 - 170)(Fanelli and Beyer 1974)	69	--	--
Gibbon	178 (120 - 300)(Fanelli and Beyer 1974)	52	--	--
Cynomolgus monkey	--	--	36 (30 - 42)(Fanelli and Beyer 1974)	10
Squirrel monkey	--	--	30 (12 - 60)(Fanelli and Beyer 1974)	15
Mouse	--	--	53 (30 - 78)(Wu, Wakamiya et al. 1994, So and Thorens 2010)	17
Rat	--	--	67 (64 - 70)(Mazzali, Hughes et al. 2001, Lu, Jia et al. 2016)	15
Dog	--	--	18(Miller, Danzig et al. 1951)	25
Mean	205 ± 75	58.9 ± 8.3	41 ± 19	16.5 ± 5.3

SUA: serum uric acid. The mean of the SUA was calculated based on reported levels. The range of SUA was included in the parenthesis.

Molecular Pharmacology Fast Forward. Published on May 2, 2018 as DOI: 10.1124/mol.117.111153
This article has not been copyedited and formatted. The final version may differ from this version.

Table 6. Kinetic parameters of [^{14}C]-uric acid uptake by hOAT1 and cyOAT1 in HEK293 cells stably expressing the transporters.

	Human	Cynomolgus Monkey
K_m (μM)	571 ± 97.7	1070 ± 90**
V_{max} (pmol/mg/min)	1510 ± 243	1040 ± 106
V_{max}/K_m (μL/mg/min)	2.6	0.97

N≥2. Student's t-test was performed to determine significant differences between the two groups. ** $P < 0.01$.

Molecular Pharmacology Fast Forward. Published on May 2, 2018 as DOI: 10.1124/mol.117.111153
This article has not been copyedited and formatted. The final version may differ from this version.

Figure 1

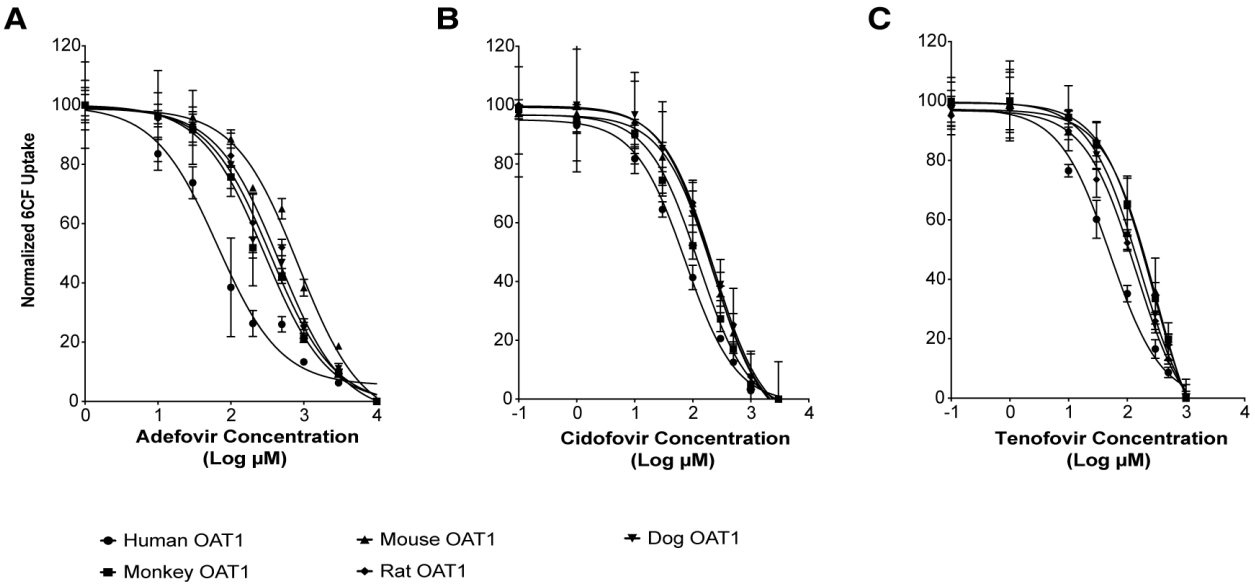

Molecular Pharmacology Fast Forward. Published on May 2, 2018 as DOI: 10.1124/mol.117.111153
This article has not been copyedited and formatted. The final version may differ from this version.

Figure 2

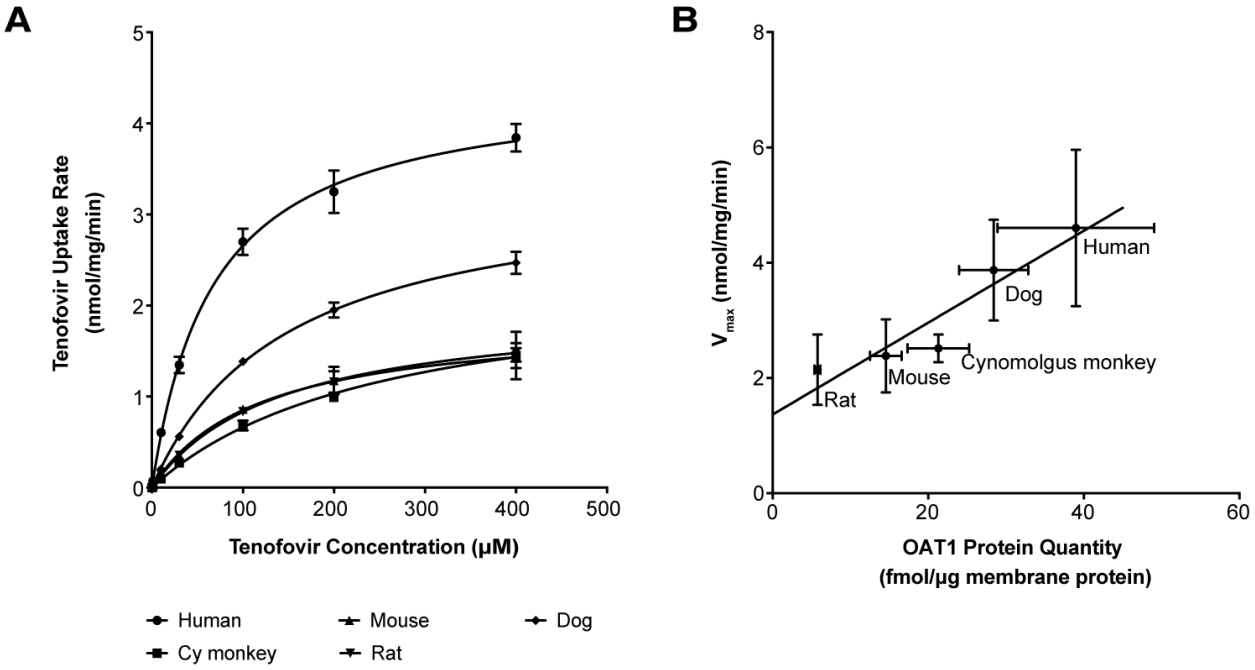

Molecular Pharmacology Fast Forward. Published on May 2, 2018 as DOI: 10.1124/mol.117.111153
This article has not been copyedited and formatted. The final version may differ from this version.

Figure 3

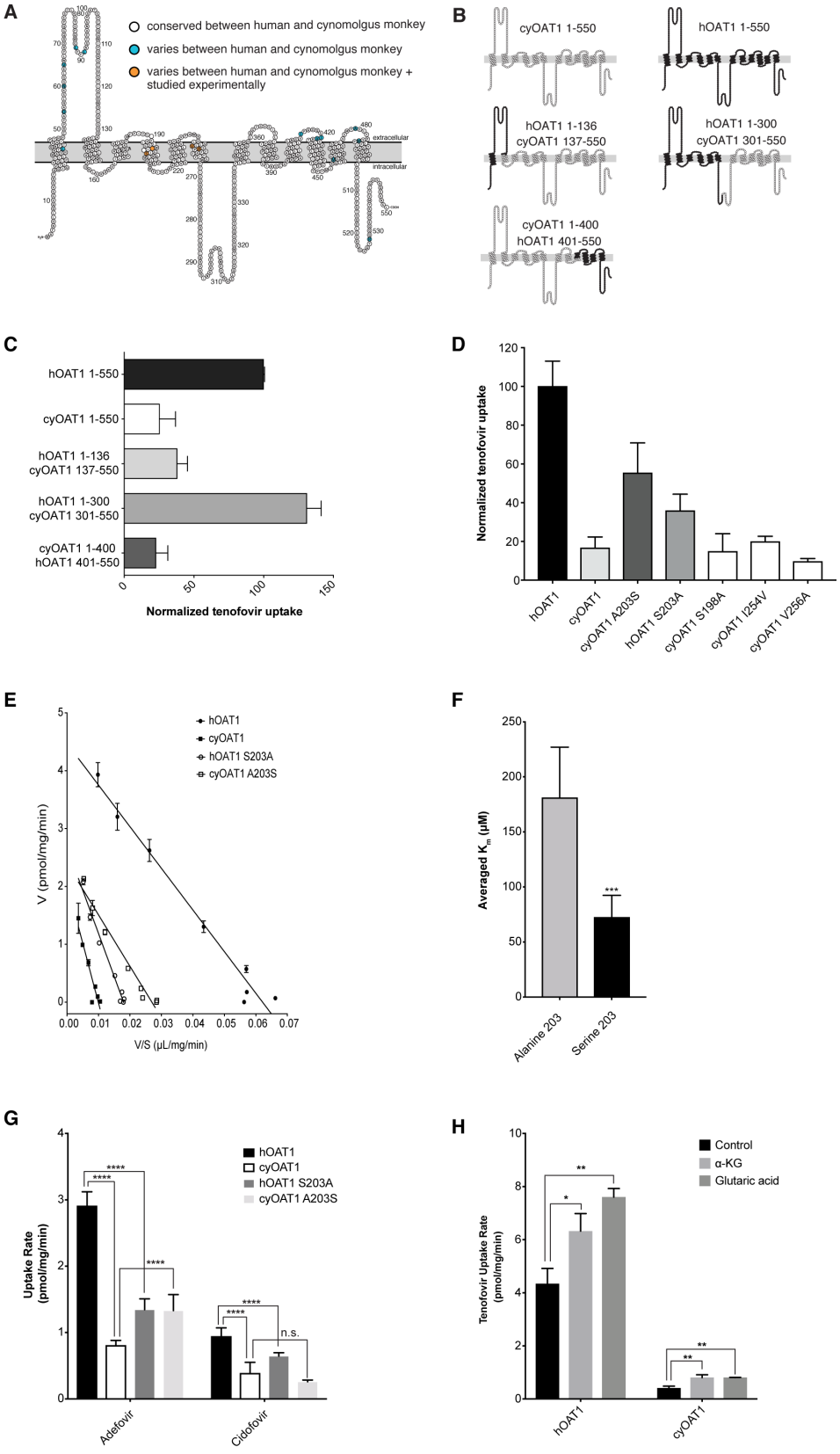

Molecular Pharmacology Fast Forward. Published on May 2, 2018 as DOI: 10.1124/mol.117.111153
This article has not been copyedited and formatted. The final version may differ from this version.

Figure 4

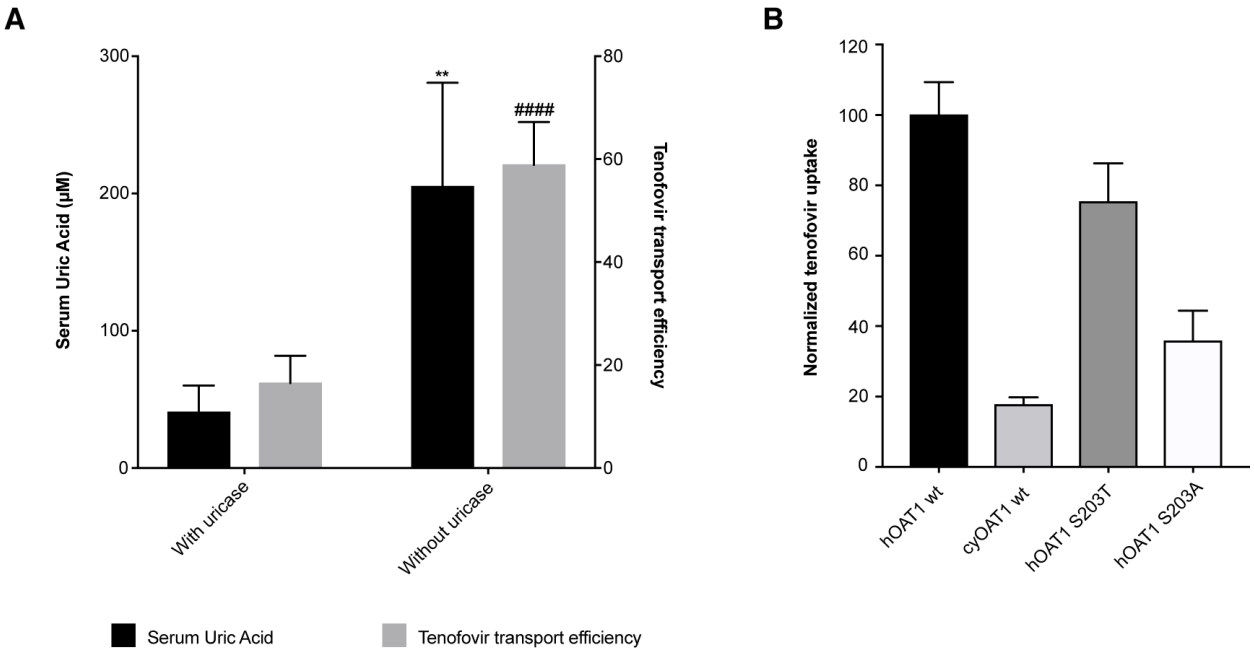

Molecular Pharmacology Fast Forward. Published on May 2, 2018 as DOI: 10.1124/mol.117.111153
This article has not been copyedited and formatted. The final version may differ from this version.

Figure 5